



Measurement report: High Contributions of Halohydrocarbon and Aromatic Compounds to Emissions and Chemistry of Atmospheric VOCs in Industrial Area

Ahsan Mozaffar^{1,2,3}, Yan-Lin Zhang^{1,2,3*}, Yu-Chi Lin^{1,2,3}, Feng Xie^{1,2,3}, Mei-Yi Fan^{1,2,3}, and Fang Cao

^{1,2,3}

5 ¹Yale-NUIST Center on Atmospheric Environment, International Joint Laboratory on Climate and Environment Change, Nanjing University of Information Science and Technology, Nanjing, 210044, China.

²Key Laboratory Meteorological Disaster; Ministry of Education & Collaborative Innovation Center on Forecast and Evaluation of Meteorological Disaster, Nanjing University of Information Science and
10 Technology, Nanjing, 210044, China.

³Jiangsu Provincial Key Laboratory of Agricultural Meteorology, College of Applied Meteorology, Nanjing University of Information Science & Technology, Nanjing 210044, China.

Correspondence to: Yan-Lin Zhang (dryanlinzhang@outlook.com)

Abstract. Volatile organic compounds (VOCs) are key components for tropospheric chemistry and air
15 quality. We investigated ambient VOCs in an industrial area in Nanjing, China from July 2018 to May 2020. The total VOCs (TVOCs) concentration was 59.8 ± 28.6 ppbv during the investigation period. About twice TVOCs concentrations were observed in autumn (83 ± 20 ppbv) and winter (77.5 ± 16.8 ppbv) seasons compared to those in spring (39.6 ± 13.1 ppbv) and summer (38.8 ± 10.2 ppbv). Unlike
20 previous studies in Nanjing, oxygenated-VOCs (OVOCs) and halohydrocarbons were measured, the observed TVOCs was about 1.5 and 3-times higher than those previously reported in the same study area and a nonindustrial suburban area in Nanjing, respectively. Observed TVOCs concentrations were similar to those in metropolitan city Beijing and Shanghai, however, it was about 1.5-3 folds higher than those in Lanzhou, Wuhan, Tianjin, Ningbo, Chengdu, London, Los Angeles, and Tokyo. Due to the industrial influence, halohydrocarbons (14.3 ± 7.3 ppbv, 24%) VOC-group was the second largest
25 contributor to the TVOCs after alkanes (21 ± 7 ppbv, 35%), which is in contrast with the previous studies in Nanjing and also in almost other regions in China. Relatively high proportions of helohydrocarbons



and aromatics were observed in autumn (25.7 and 19.3%, respectively) and winter (25.8 and 17.6%, respectively) compared to those in summer (20.4 and 11.8%, respectively) and spring (20.3 and 13.6%, respectively). According to the potential source contribution function (PSCF), short-distance transports from the surrounding industrial areas and cities were the main reason for high VOC concentration in the study area. According to positive matrix factorization (PMF) model results, industry-related sources (23-47%) followed by vehicle emissions (24-34%) contributed the major portion to the ambient VOC concentrations. Whereas aromatics followed by alkenes were the top contributors to the loss rate of OH radicals (L^{OH}) (37 and 32%, respectively), alkenes followed by aromatics contributed most to the ozone formation potential (OFP) (39 and 28%, respectively). Besides, the aromatics VOC-group was also the major contributor to the secondary organic aerosol potential (SOAP) (97%). According to the empirical kinetic modelling approach (EKMA) and relative incremental reactivity (RIR) analysis in assistance with a photochemical box model, the study area was in the VOC-sensitive regime for ozone (O_3) formation during all the measurements seasons. Therefore, mainly alkenes and aromatics emissions chiefly from industries and automobiles should be reduced to decrease the secondary air pollution formation in the study area.

1 Introduction

Air pollution characterized by severe ozone (O_3) and haze pollution is a big problem in urban and industrial areas in China (He et al., 2019; Hui et al., 2018; Tan et al., 2018; Jia et al., 2016; Feng et al., 2016; Hui et al., 2019). In recent years, O_3 concentration above the national standard, and severe haze events are frequently reported (He et al., 2019; Hui et al., 2019; Sheng et al., 2018; Feng et al., 2016; Tan et al., 2018; Jia et al., 2016). As a precursor of O_3 and secondary organic aerosol (SOA), volatile organic compounds (VOCs) are largely responsible for the severe air pollution in China (Song et al., 2018; Hui et al., 2019; Hui et al., 2018; He et al., 2019). Unfortunately, anthropogenic VOC emissions have been increasing over the last 2 decades in China and it is expected to do so in the future (Mozaffar & Zhang, 2020, and references therein).

Atmospheric VOC has plenty of sources; it can be emitted from various anthropogenic and biogenic sources. Besides, it can also be formed in the atmosphere. Anthropogenic VOC sources mainly include



industrial emission, vehicle exhaust, solvent usages, biomass burning, and fuel evaporation. On the
55 other hand, vegetation is the main biogenic sources of VOC. In developed areas in China, vehicle
exhaust and industrial emission are the 2 major VOC sources (He et al., 2019; Hui et al., 2018; Hui et
al., 2019; Mo et al., 2017; Song et al., 2018; An et al., 2014; Mozaffar & Zhang, 2020). Whereas
vehicle-related sources are more dominant in the North China Plain (NCP), Central China (CC), and
Pearl River Delta region (PRD), industry-related sources are more influential in the Yangtze River Delta
60 (YRD) area (Zhang et al., 2017; Meng et al., 2015; Sun et al., 2019; He et al., 2019; Zhang et al., 2018;
An et al., 2017; Mozaffar & Zhang, 2020; Shao et al., 2016). Alkanes, Alkenes, aromatics, oxygenated-
VOCs (OVOCs), and halohydrocarbons are the most common VOC-groups in the atmosphere (Hui et
al., 2019; Hung-Lung et al., 2007; Song et al., 2018; Tiwari et al., 2010; He et al., 2019; Na et al., 2001;
Hui et al., 2018). VOC concentration and composition changes depending on seasons, for example, the
65 contribution from biogenic and solvent utilization increases in summer, and contribution from
combustion sources increases in winter (Mo et al., 2017; Song et al., 2018; An et al., 2014). The
chemical reactivity of VOC depends on its chemical composition, for instance, alkenes and aromatics
are generally more reactive than alkanes (Carter, 2010). To understand the chemical reactivity and
secondary product formation ability of VOCs, analysis of OH radical loss rate (L^{OH}), ozone formation
70 potential (OFP), and secondary organic aerosol potential (SOAP) are commonly used (Song et al., 2018;
He et al., 2019; Hui et al., 2018; Hui et al., 2019).

Industries are an important source of VOC, and different reactive and hazardous VOCs emissions from
industries are already reported in different areas on earth (Zhang et al., 2018; Na et al., 2001; Hung-
Lung et al., 2007; Yan et al. 2016; Tiwari et al., 2010; Shi et al., 2015; Zhang et al., 2018b). For
75 instance, Zhang et al. (2018) reported a high concentration of alkanes (82%) and lifetime cancer risk of
different aromatics and halohydrocarbons in a petroleum refinery in Guangzhou, China. A high
concentration of OVOCs (63%) was observed in an industrial area in Ulsan, Korea (Na et al., 2001).
Hung-Lung et al.(2007) mentioned a high concentration of aromatics in an industrial area in Taiwan. A
high concentration of halohydrocarbons (49%) was observed in an iron smelt plant in Liaoning, China
80 (Shi et al., 2015). Zhang et al. (2018) mentioned a high concentration of alkanes (42%) and aromatics
(20%) in a petrochemical and other industries affected area in Shanghai, China. High concentrations of



aliphatic and aromatics were observed in a petrochemical industrial area in Yokohama, Japan (Tiwari et al., 2010). Therefore, VOC composition varied among the industries/industrial areas in different regions. Mostly short-term investigations were performed to characterize the VOCs in industry-affected areas. In the current study, we carried out a comprehensive investigation on VOC in an industrial area in Nanjing between July 2018 and May 2020. Nanjing is located in the YRD region which is mainly affected by industrial emissions. Several VOC investigations have already been performed in the Nanjing industrial area but OVOCs and halohydrocarbons were not measured in those studies (An et al., 2017; An et al., 2014). However, OVOCs and halohydrocarbons are already mentioned as one of the highest concentrated VOC-groups in other industrial regions (Na et al., 2001; Shi et al., 2015). In the current study area, a high concentration of alkanes (45%) and alkenes (25%) were observed in a previous investigation (An et al., 2014). Besides the incomplete VOC measurements, O₃ formation sensitivity to its precursors was not investigated properly using a photochemical box model in Nanjing. Moreover, source apportionment of VOCs was not conducted for different seasons of a year.

95

In the current study, we report the variations in concentrations and compositions of VOC during the observation period. We present the possible source areas and potential sources of VOC based on potential source contribution function (PSCF) and positive matrix factorization (PMF) model analysis. We also present the contributions of different sources to ambient VOC during the measurement period. We report the chemical reactivity and secondary product formation capacity of the VOC using L^{OH}, OFP, and SOAP analysis. We also present the sensitivity analysis of O₃ formation using empirical kinetic modelling approach (EKMA) and relative incremental reactivity (RIR) analysis. Therefore, this study provides valuable information to the scientific community and policymakers.

2 Material and Methods

2.1 Sampling Site Description, Gases Analysis, and Meteorology Data

Field measurements were carried out from July 2018 to May 2020 at Nanjing University of Information Science and Technology (32.1°N, 118.4°E), which is located in an industrial area in Nanjing, China.



The sampling site was on the rooftop of a building (~20 m). The sampling site is surrounded by different chemical and petrochemical industries, steel plants, gas stations, high traffic roads, and residential areas. A detailed description of the sampling site can be found elsewhere (Mozaffar et al., 2020).

We analysed ambient air VOCs using an online GC-FID/MS instrument (AC-GCMS 1000, Guangzhou Hexin Instrument Co., Ltd., China). FID detector analysed C2-C5 VOCs and MS analysed C6-C12 VOCs. The instrument analysed one sample at every hour. During the investigation period, we inspected and calibrated the instrument regularly to ensure the accuracy of the data. We monitored the O₃ concentrations using a 49i O₃ analyser (Thermo Fisher Scientific Inc., USA), NO, NO₂ and NO_x concentrations were measured using a 42i NO-NO₂-NO_x analyser (Thermo Fisher Scientific Inc., USA), SO₂ concentrations were followed using a 43i SO₂ analyser (Thermo Fisher Scientific Inc., USA), and CO concentrations were measured using a 48i CO analyser (Thermo Fisher Scientific Inc., USA). We also measured temperature and relative humidity, wind speed, wind direction, and solar radiation by HMP155 (Vaisala, Finland), 010C (Met One Instruments, Inc., USA), 020CC (Met One Instruments, Inc., USA), and CNR4 (Kipp & Zonen, The Netherlands) analysers, respectively. A detailed description of the instrumentation, sampling procedure, analysis, quality control, and calibration procedure can be found elsewhere (Mozaffar et al., 2020).

2.2 Positive Matrix Factorization (PMF) model and Potential Source Contribution Function (PSCF)

We used the positive matrix factorization (PMF) model (US Environmental Protection Agency, USEPA, version 5.0) for the source apportionments of VOCs. A detailed description of the model can be found elsewhere (Hui et al., 2019; Song, Tan, Feng, Qu, Liu, et al., 2018). In this study, we used 62 potential VOC tracers (Fig. S1 - S4) in the PMF model to analyse the VOC sources for different seasons. The error fraction was set to 20% for the sample data uncertainty estimation. We explored the PMF factor number from 4-8 to determine the optimal number of sources. Finally, we decided to choose an 8-factor solution ($Q_{\text{true}}/Q_{\text{robust}} = \sim 1.0$).

We used the potential source contribution function (PSCF) to locate possible source areas of VOCs for different seasons during the investigation period. We used Zefir analysis software to do the PSCF



analysis and the Hysplit4 model to cluster the backward trajectories (Petit et al., 2017). Backward trajectories in the sampling site were estimated using the data provided by the National Centers for Environmental Prediction (<ftp://arlftp.arlhq.noaa.gov/pub/archives/gdas1>). We estimated 24 hr backward trajectories 24 times a day arriving at 500 m above the ground surface using the hysplit4 model. For the PSCF analysis, we divided the geographic region covered by the back trajectories into an array of $0.1^\circ \times 0.1^\circ$ grid cells and used the mean TVOCs concentration as the VOC reference value. More details about the PSCF analysis can be found in previous studies (Chen et al., 2018).

2.3 OH radical loss rate (L^{OH}), Ozone formation potential (OFP), and Secondary organic aerosol potential (SOAP)

To evaluate the daytime photochemistry of VOCs, we estimated their OH radical loss rate (L^{OH}). The following equation was used to estimate the L^{OH} (s^{-1}) (Zhang et al., 2020).

$$L^{\text{OH}} = [\text{VOC}]_i \times K_i^{\text{OH}} \quad (1)$$

Where $[\text{VOC}]_i$ is the concentration of VOC species i (molecule cm^{-3}), K_i^{OH} ($\text{cm}^3 \text{ molecule}^{-1} \text{ s}^{-1}$) is the reaction rate constant of i VOC with OH radical. The K^{OH} values for the VOCs are collected from Carter (2010) (Table S1).

The Ozone formation potential (OFP) of the VOCs is their maximum contribution to the O_3 formation (Hui et al., 2018a). The OFP (ppbv) of the VOCs was estimated using the following equation.

$$\text{OFP} = [\text{VOC}]_i \times \text{MIR}_i \quad (2)$$

Where MIR_i is the maximum incremental reactivity of the i VOC. The MIR values for the VOCs are also collected from Carter (2010) (Table S1).

The contribution of VOCs to the formation of secondary organic aerosol is estimated by secondary organic aerosol potential (SOAP) (Song et al., 2018). We estimated the SOAP (ppbv) of VOCs using the following equation.

$$\text{SOAP} = [\text{VOC}]_i \times \text{SOAP}_i^p \quad (3)$$



Where $SOAP_i^P$ is the SOA formation potential of the i VOC on a mass basis relative to toluene (Derwent et al., 2010). In this study, the $SOAP^P$ factors of the VOCs are collected from Derwent et al. (2010) (Table S1).
165

2.4 Empirical Kinetic Modelling Approach (EKMA) and Relative Incremental Reactivity (RIR)

The empirical kinetic modelling approach (EKMA) is a well-known procedure to develop the O_3 formation reduction strategy by testing the relationship between ambient O_3 and its precursors (He et al., 2019; Hui et al., 2018; Vermeuel et al., 2019; Tan et al., 2018). In this study, we used the Framework for 0-D Atmospheric Model (FOAM v 3.2, Wolfe et al., 2016), a photochemical box model run by Master Chemical Mechanism (MCM) v3.2 chemistry (Jenkin et al., 1997; 2003, 2015; Saunders et al., 2003), to get the data for the EKMA isopleth. The FOAM-MCM box model can simulate 16940 reactions of 5733 chemical species. The box model was run using the VOCs and gas concentrations and the meteorological data as input. To generate the O_3 isopleth from the model simulated data, a total of 175 121 reduction scenarios (11 NO_x \times 11 VOC) were simulated and the maximum O_3 produced in each scenario was saved.

The O_3 formation sensitivity to its precursors' concentrations can also be assessed by the relative incremental reactivity (RIR, Cardelino & Chameides, 1995). We also utilized the FOAM-MCM box model data to estimate the RIR. The RIR is simply defined as the percentage change in O_3 formation per percentage change in precursor's concentration. In this study, we reduced the precursor's concentration by 10% for the RIR estimation. The RIR was estimated using the following equation.
180

$$RIR(X) = \frac{[P_{O_3}(X) - P_{O_3}(X - \Delta X)] / P_{O_3}(X)}{[\Delta X] / [X]} \quad (4)$$

Where $[X]$ is the observed concentration of a precursor X , $[\Delta X]$ is the changes in the concentration of X . $P_{O_3}(X)$ and $P_{O_3}(X - \Delta X)$ are the simulated net O_3 production with the observed and the reduced concentration of the precursor X , respectively.
185



3 Results and discussion

3.1 Overview of the metrological conditions and air pollutants concentrations

The time series of the hourly inorganic air pollutants, meteorological parameters, and TVOC concentrations are shown in Fig. 1. The discontinuity of the time series data is due to the failure of the instruments. The measured data from July to August 2018, September to November 2018, December 2018 to January 2019, and April to May 2020 are termed as summer, autumn, winter, and springtime data, respectively. Overall, the observed temperature and solar radiation gradually decreased from summer to winter and increased back to the summertime level in spring. The temperature ranged between -5.7 and 41.4 °C during the measurement period. The relative humidity values varied from 18 to 100% and high values were generally observed in winter and autumn. During the observation period, wind speed ranged between 0.1 and 7.5 ms^{-1} . Wind prevailed at the sampling site from many directions during the measurement periods; more details about the wind direction will be discussed in Sect.3.3.2. The O_3 and NO_x concentrations varied from 2 to 160 ppbv and 0.4 to 90 ppbv, respectively. Whereas high O_3 concentrations (>80 ppbv) were observed in summer and spring, high NO_x concentrations were measured in winter and at the end of autumn. The CO and SO_2 concentrations ranged from 83 to 3398 ppbv and 0.5 to 21 ppbv, respectively. Generally, high concentrations of CO and SO_2 were observed in winter and spring. The measured NO and NO_2 concentrations varied from 0.4 to 51 ppbv and 1 to 79 ppbv, respectively. In general, the high NO and NO_2 concentrations were observed in autumn and winter. The TVOCs concentrations varied between 9 and 393 ppbv during the observation period and the high values were measured in autumn and winter. More details about the abovementioned parameters will be discussed in the following section.

3.2 Concentration and composition of VOCs

In total 100 VOCs were observed in Nanjing industrial area, including 27 alkanes, 11 alkenes, 1 alkyne, 17 aromatics, 31 halohydrocarbons, 12 OVOCs, and 1 other (carbon disulfide) (Table S2). Ethane (5.8 ± 2.5 ppbv), propane (4.2 ± 1.5 ppbv), and ethylene (3 ± 1.6 ppbv) were the most abundant VOCs in the study area during the observation period. However, we observed season-wise variations in the order of abundant VOC species (Table S2). For instance, acetone was the 3rd highest concentrated VOC in



spring. The abovementioned 4 VOC species are also frequently mentioned as the most abundant VOCs in different regions in China (Deng et al., 2019; He et al., 2019; J. Li et al., 2018; Ma et al., 2019). We
215 compared the individual VOC concentrations with the available data presented in recent investigations. The individual VOC concentrations in the current observation were similar to those in the previous investigations in the same study area, however, they were almost twice of those found in a nonindustrial suburban area in Nanjing (Table S2). The individual VOC concentrations in the current observation were about 1.4 fold lower than those in Beijing (Li et al., 2015) and Shanghai (Zhang et al., 2018), but,
220 similar to those measured in Guangzhou (Zou et al., 2015). During the observation period, the concentrations of different VOC-groups were in the order of alkanes (21 ± 7 ppbv, 35%)> halohydrocarbons (14.3 ± 7.3 ppbv, 24%)> aromatics (9.9 ± 5.8 ppbv, 17%)> OVOCs (7.5 ± 1.9 ppbv, 13%)> alkenes (5 ± 1.9 ppbv, 8%)> alkynes (1.4 ± 0.3 ppbv, 2%)> others (0.5 ± 0.2 ppbv, 1%). However, we noticed relatively higher proportions of OVOCs (14% and 18%) than the aromatics (12% and 14%)
225 in summer and spring (Fig. 2c & f). The relatively higher contribution of OVOCs in summer and spring could be related to the biogenic emissions (e.g. acetone, MEK from trees). Indeed, the relative contribution of acetone and MEK to the TVOCs were higher in summer and spring than those in autumn and winter (Table S2). Huang et al. (2019) reported that the industries, biogenic emissions, and secondary formation are the main source of OVOCs in southern China. Relatively high proportions of
230 halohydrocarbons and aromatics were observed in autumn (25.7 and 19.3%, respectively) and winter (25.8 and 17.6%, respectively) compared to those measured in summer (20.4 and 11.8%, respectively) and spring (20.3 and 13.6%, respectively) (Fig. 2f). The high proportions of halohydrocarbons and aromatics in autumn and winter could be related to the burning of biomass and fossil fuel for additional heating. Similar to the observation in the current study, the alkane is generally the most abundant VOC
235 group in China (Mozaffar & Zhang, 2020). The relatively high contribution from halohydrocarbons to the TVOCs could be related to the industrial emissions in the study area. In previous studies in an iron smelt plant in Liaoning, China, a high concentration of halohydrocarbons (49%) was observed (Shi et al., 2015). However, halohydrocarbons were not measured in previous investigations in the same study area (An et al., 2014; An et al., 2017; Shao et al., 2016) and also in another suburban area in Nanjing
240 (Wu et al., 2020). Either aromatics or alkenes was mentioned as the second most abundant VOC-group



in those studies in Nanjing, which is the 3rd and 5th most abundant VOC group in the current investigation. In Shanghai, a nearby city, alkanes (42%) and alkenes (26%) were two major VOC-groups (Zhang et al., 2018). The TVOCs concentration was 59.8 ± 28.6 ppbv over the whole observation period, and relatively higher TVOCs concentrations were measured in autumn (83 ± 20 ppbv) and winter (77.5±16.8 ppbv) compared to those in spring (39.6 ± 13.1 ppbv) and summer (38.8 ± 10.2 ppbv). About 1.5-times higher TVOCs concentration was observed relative to the previous investigation in the same study area (An et al., 2014; An et al., 2017). Besides, we also found 3-times higher TVOCs concentration compared to the one in a nonindustrial suburban area in Nanjing (Wu et al., 2020). Halohydrocarbons and OVOCs were not measured in those previous studies in Nanjing, it could be one of the reasons for the relatively high TVOCs concentration in the current study. Observed autumn and wintertime TVOCs concentrations were similar to those measured in urban Beijing (86.2 ppbv in autumn) and Shanghai (94.1 ppbv in winter) (Li et al., 2015; Zhang et al., 2018). Similarly, observed summertime TVOCs concentration was similar to those found in urban Xi'an (42.6 ppbv), Wuhan (43.9 ppbv) (Zeng et al., 2018; Sun et al., 2019). However, yearly TVOCs concentration was 1.5-3 folds higher than those in Lanzhou, Wuhan, Tianjin, Ningbo, Chengdu, London, Los Angeles, and Tokyo (Jia et al., 2016; Hui et al., 2018; B. Liu et al., 2016a; Mo et al., 2017; Song et al., 2018; von Schneidemesser et al., 2010; Warneke et al., 2012; Hoshi et al., 2008). The diurnal variation of the TVOCs, alkenes, aromatics, halohydrocarbons, OVOCs, and alkanes concentrations showed a double-hump structure (Fig. 2a, b, d, & e). This double-hump pattern indicates the contribution of traffic emission during the rush-hours in the morning and evening. The lowest concentration of the TVOCs and different VOC-groups reached 12:00-16:00. Oppositely, the highest concentration of O₃ reached at that period (Fig. 3). The lowest O₃ concentrations were observed in winter which was consistent with the solar radiations.

3.3 Sources of VOCs

3.3.1 Specific Ratios

The use of the toluene/benzene (T/B) ratio is one of the simplest ways to preliminary analyse the VOC sources. If the T/B ratio is < 2 , the study area is mainly affected by vehicle emissions (Hui et al., 2018,



2019). If the T/B ratio is > 2 , the study area is influenced by other sources (e.g. industry, solvent utilization) beside vehicle emissions (Kumar et al., 2018; Niu et al., 2012; Li et al., 2019). Moreover, the T/B ratios are ranged between 0.2-0.6 in coal and biomass burning affected areas (Wang et al., 2009; Akagi et al., 2011). The diurnal variations in T/B ratios during different seasons are depicted in Fig. 4 (a, b, c, & d). The mean values of T/B ratios were ranged between 0.9-2 (1.4 ± 0.3), 1.3-2 (1.7 ± 0.2), 1.1-1.6 (1.4 ± 0.1), and 1.4-2.7 (1.9 ± 0.3) during summer, autumn, winter, and spring, respectively. As the mean values of T/B ratios were around 2, the study area could be mainly affected by vehicle emissions. The double-hump pattern in the diurnal variations in T/B ratios also indicates that the rush-hour traffic had a significant influence on the VOCs concentrations in the study area. Besides, the 75th percentiles of T/B ratios were above 2 most of the investigation periods, therefore, the study area could also be influenced by industrial emissions.

Figure 4 (e, f, g, & h) shows the ratios of different alkanes and aromatics to acetylene. Acetylene is a tracer of combustion sources, the ratios of different alkanes and aromatics to acetylene are used to comprehend the contribution of other sources to combustion sources. The mean ratios of propane, n-butane, and i-butane to acetylene were around 2.0-4.0, 0.7-1.6, and 0.4-0.8, respectively during all the seasons, which were smaller than those (11.5, 1.8, and 2.6, respectively) observed in Guangzhou city centre, which was affected by liquefied petroleum gas (LPG) emissions (Zhang et al., 2013). Therefore, LPG usages probably contributed a little fraction to the alkanes in the study area. The mean ratios of benzene, toluene, C8-aromatics, and C9-aromatics to acetylene were around 0.3-1.0, 0.4-1.1, 0.2-0.6, and 0.1, respectively during all the seasons. The observed ratios of benzene and toluene to acetylene were much higher than those found in Jianfeng Mountains in Hainan (0.2 and 0.1, respectively) but comparable to those measured in urban Guangzhou (0.4 and 0.4-1, respectively) (Tang et al., 2007). Besides, the observed ratios of C8-aromatics and C9-aromatics to acetylene were comparable to traffic emission influenced urban Guangzhou (0.68 and 0.2, respectively) and Wuhan (0.5 and 0.2, respectively) (Zhang et al., 2013; Hui et al., 2018). Therefore, vehicle exhaust probably contributed significantly to the aromatics in the study area.



3.3.2 Potential Source Contribution Function (PSCF)

295 Besides the local sources, both the long and short distance transport of air mass could bring VOCs to the study area. Figure 5 shows the wind cluster and PSCF analysis results for different seasons. During summer, the major air masses were short-distance transports from the southwest (40%) and southeast (39%) directions. A minor air mass (21%) was transported from the east direction. High PSCF values were in the nearby southwest, southeast, and east directions; therefore, VOC pollution in the study area was mainly affected by the short-distance transport from the south and east directions. During autumn, the dominant air masses were short-distance transport from the northeast (59%) and northwest (30%) directions. However, according to the PSCF analysis, VOC pollution was mainly influenced by the short distance transport from the south and east directions. During winter, short-distance transports from the northeast (46%) and northwest (37%) directions were the major incoming air masses to the study area. According to the PSCF values, the short-distance air masses from the south and east directions were mainly transported VOC to the receptor site. During spring, air mass was mainly transported from the southwestern (49%) and eastern (30%) directions. Atmospheric VOCs to the study area were mainly transported by these two air masses mostly from the nearby areas. Overall, the high PSCF values were concentrated around the measurement site, therefore, short distance transports from the surrounding areas and cities were the main reason for the high VOC concentration. The above conclusion perfectly makes sense as the sampling site is surrounded by different chemical and petrochemical industries, steel plants, gas stations, high traffic roads, and residential areas.

3.3.3 PMF Model Analysis

Differences were observed among the source profiles of VOCs obtained for different seasons (Sect. S1). For instance, the biogenic source was identified in summer, biomass burning source was distinguished in autumn, and LPG/NG usage source was found in winter and spring. However, industry and vehicle-related VOC sources were identified during all the measurement seasons. According to PMF model results, aromatics were emitted from solvent usages, vehicle, and industry-related sources. Besides, industry and combustion processes were the main sources of halohydrocarbons and OVOCs. Moreover, alkanes and alkenes were emitted from vehicle exhaust and fuel usage sources.



Figure 6 shows the relative contributions of different sources to ambient VOCs during different seasons. Overall, industry-related sources contributed to the major portion of the ambient VOC concentrations followed by vehicle emission. Industrial emission accounted for about 32%, 47%, 45%, and 23% in summer, autumn, winter, and spring, respectively. The contributions of vehicle emission were about 34%, 26%, 24%, and 27% in summer, autumn, winter, and spring, respectively. The contribution of vehicle emission remained similar during the 4 seasons, however, the contribution of the industrial emission increased in autumn and winter. Previous investigations performed in Beijing, Tianjin, Wuhan, Chengdu, and Shuozhou also found that the industry and vehicle are the two most important VOC sources (Zhang et al. 2017; Liu et al. 2016; Hui et al. 2018; Song et al. 2018) Jia et al., 2016). Besides these two sources, solvent usage (11%, 10%, 10%, and 4%, respectively) and gasoline evaporation (17%, 10%, NA, 6%, respectively) were two important VOC sources during those 4 seasons. Moreover, source contribution from the biogenic source in summer (7%), biomass burning in autumn (7%), LPG/NG usage in winter (11%) and spring (18%), and multiple sources in winter (10%) and spring (23%) was observed.

3.4 Chemical reactivity (L^{OH}) and contribution to O_3 and SOA formation

The estimated loss rates of OH radical (L^{OH}) with VOCs were about 2-fold high in autumn (13.7 s^{-1}) and winter (13.5 s^{-1}) compared to those in summer (7 s^{-1}) and spring (7.5 s^{-1}) (Fig. 7 a). The relatively high L^{OH} values in autumn and winter were due to the relatively high VOC concentrations in those seasons (Fig.2). The average L^{OH} value was $10.4 \pm 3.6 \text{ s}^{-1}$ over the four seasons. It was in a similar range with the values determined in Guangzhou (10.9 s^{-1}), Chongqing (10 s^{-1}), Xian ($1.6\text{-}16.2 \text{ s}^{-1}$), and Tokyo ($7.7\text{-}13.4 \text{ s}^{-1}$), however, higher than the values estimated in Shanghai ($2.9\text{-}5 \text{ s}^{-1}$, 6.2 s^{-1}) and Beijing (7 s^{-1}) (Tan et al., 2019; Zhu et al., 2019; Yoshino et al., 2012; Song et al., 2020). While alkene was the highest contributor to the L^{OH} in summer (3 s^{-1} , 43%) and spring (2.6 s^{-1} , 35%), aromatic was the maximum contributor in autumn (6.9 s^{-1} , 50%) and winter (5.9 s^{-1} , 44%) (Fig. 11 a & d). An increase in the OH loss rate by OVOCs was observed in spring (17%) compared to the other seasons (10, 8, and 9% in summer, autumn, and winter, respectively). Over the four seasons, the contribution of VOC-groups to



L^{OH} exhibited the following trend: aromatics > alkenes > alkanes > OVOCs > halohydrocarbons. Similar to the current study, aromatic is also mentioned as the maximum contributors to L^{OH} in different regions in China, however, the alkene is generally reported as the top contributor to L^{OH} (Zhang et al.,
350 2020; Zhao et al., 2020; Hui et al., 2018; Song et al., 2020). Figure 7 also shows the top 10 VOCs contributing to L^{OH} for different seasons. Whereas isoprene was the highest contributor to L^{OH} in summer, styrene was the largest contributor in autumn and winter. On the other hand, naphthalene was the main contributor to L^{OH} in spring. Overall, styrene, naphthalene, ethylene, and isoprene were the
355 main contributor to L^{OH} in the study area. In previous studies in China, these compounds are also mentioned as one of the highest contributors to L^{OH} (Zhao et al., 2020; Hui et al., 2018; Song et al., 2020).

The estimated O_3 formation potential (OFP) of VOCs were about 2-times high in autumn (170.8 ppbv) and winter (175.4 ppbv) relative to those in summer (86.2 ppbv) and spring (82.8 ppbv) (Fig. 8 a). The
360 average OFP value was 128.8 ± 51.2 ppbv during the measurement period. The springtime OFP was similar to the one estimated in Beijing (80 ppbv) (Li et al., 2015). The summertime OFP was about 1.5 times higher than the one in Xi'an (Song et al., 2020), but, about 1.4-2 folds lower than those found in Shanghai (Liu et al., 2019). The average OFP was about 1.5 times higher than the one in Wuhan (Hui et al., 2018). Whereas alkene was the major contributor to OFP in summer (37.4 ppbv, 43%), winter
365 (72.8 ppbv, 41%), and spring (31.6 ppbv, 38%), aromatics contributed the most to OFP in autumn (62.7 ppbv, 37%) (Fig. 12 a & d). During the measurement period, the contribution of VOC-groups to OFP showed the following trend: alkenes > aromatics > alkanes > OVOCs > halohydrocarbons. The alkene is also mentioned as the top contributor to OFP in Nanjing and the same observation is commonly found in China (An et al., 2014; Hui et al., 2018; Song et al., 2018; Song et al., 2020). The top 10 VOCs
370 contributing to OFP for different seasons are also shown in Fig. 8 (b, c, e, & f). Ethylene was the major contributor to OFP during all the season. Followed by ethylene, cis-1,3-dichloropropene was the main contributor to OFP from summer to winter. In spring, propylene was the second most contributors to OFP. Overall, different alkenes were the highest contributor to OFP in the study area. Alkenes are also mentioned as the top contributor to OFP in the previous investigations in Nanjing (An et al., 2014).



375 Therefore, the reduction of these alkenes emissions in the study area could be one of the ways to reduce ambient O₃ concentration.

The secondary organic aerosol potentials (SOAP) were about 3-times higher in autumn (1422 ppbv) and winter (1269 ppbv) than those in summer (466 ppbv) and spring (398 ppbv) (Fig. 9a). The average SOAP was 889±531 ppbv during the measurement period. The average SOAP was about 2-3 times
380 higher than those estimated in Wuhan and Beijing (Hui et al., 2019; Li et al., 2020). Aromatics was the main contributor to SOAP during all the seasons (95-97%) (Fig. 9 a & d) which was consistent with the observations in Chengdu (Song et al., 2018), Beijing (Li et al., 2020), and Wuhan (Hui et al., 2019). During the measurement period, the contribution of VOC-groups to SOAP exhibited the following trend: aromatics > alkanes > alkenes > OVOCs. Styrene, cumene, toluene, benzene, and o-xylene were
385 the major contributor to SOAP during all the season (Fig. 9 b, c, e, & f). Therefore, the reduction of these aromatics emissions in the study area could be one of the ways to reduce ambient SOA concentration.

3.5 Sensitivity analysis of O₃ formation

Figure 10 shows the EKMA isopleth diagrams of O₃ for different seasons. In all the diagrams, VOC and
390 NO_x = 100 % is the base case. The ridgeline divided the diagrams into two regimes, VOC-sensitive (above) and NO_x-sensitive (below) regimes. For all the seasons, the study area fell above the ridgeline. Moreover, a decrease in O₃ production was noticed with the decrease in VOC concentration. Therefore, the study area was in the VOC-sensitive regime for O₃ formation during all the seasons. As a case study, O₃ formation sensitivity to its precursors was tested on a high O₃ concentration day (July 29
395 2018, maximum 126 ppbv). During the high O₃ episode, the study area was also in the VOC-sensitive regime for O₃ formation (Fig. S5). We also employed the RIR analysis to evaluate the O₃ production sensitivity to VOC, NO_x, and CO concentrations (Fig. 11). The RIR value of VOC was the highest during all the seasons. It indicates that the O₃ production was more sensitive to the reduction of VOC concentration. This finding is consistent with the above results in the EKMA isopleth (Fig. 10). Except
400 for the spring, the RIR values of CO were very small relative to those for the VOC. It indicates that the CO concentrations were relatively less important for the O₃ formation during those seasons. The RIR



values for NO_x were negative during all the seasons, implying that the O₃ formation was in the NO_x-titration regime in the study area. From the above analysis, it is evident that a reduction of VOC concentration in the study area will be the most efficient way to reduce the O₃ formation. The previous
405 two studies performed in Nanjing also concluded the same finding based on VOC/NO_x ratios and RIR analysis (An et al., 2015; Xu et al., 2017). Our findings are also consistent with the previous studies performed in other regions in China (Tan et al., 2018a; He et al., 2019; Feng et al., 2019; Ma et al., 2019). However, NO_x-sensitive regions for O₃ formation are also found in China (Tan et al., 2018; Jia et al., 2016).

410 **4 Conclusions**

Industries are an important anthropogenic source of VOCs. VOC plays a major role in tropospheric chemistry and air quality. Nanjing is one of the biggest industrial cities in China. We performed a long term investigation of ambient VOCs in an industrial area in Nanjing. About 1.5 and 3-folds high TVOCs concentrations were observed compared to those previously reported in the same study area and
415 a nonindustrial suburban area in Nanjing, respectively. The relatively high TVOCs was due to halohydrocarbons and OVOCs concentrations were not measured in those previous studies in Nanjing. Therefore, halohydrocarbons and OVOCs were an important part of the TVOCs in Nanjing, and industrial emissions had a large influence on VOC concentration in the study area. Observed TVOCs concentration was also about 1.5-3 folds higher than those reported in other cities in China and the
420 world, but, similar to those measured in urban Beijing and Shanghai. This high VOC concentration in the study area needs to be reduced to decrease O₃ concentration and improve the local air quality. TVOCs concentrations were about 2-times high in autumn and winter compared to those in summer and spring. Generally, haze pollutions frequently happen in autumn and winter, therefore, VOC concentration reduction in these seasons is an important step to reduce haze pollutions in the study area.
425 After alkane, halohydrocarbon was the 2nd largest contributor to the TVOCs, indicating a high influence of industrial emissions. Generally, alkenes/aromatics/OVOCs are the 2nd largest contributor to the TVOCs in China, therefore, industries in Nanjing emitted a high amount of halohydrocarbons into the atmosphere. As halohydrocarbons are carcinogenic, their emissions should be reduced. PSCF analysis



indicated that the short distance transports from the surrounding areas and cities were the main reason
430 for high VOC concentration in the study area. Hence, local emissions should be reduced to decrease the
haze and O₃ pollution in the study area. Industries were the major VOC sources in the study area
followed by vehicles, thus, emission reduction from these two sources should get more priority.
Aromatics and alkenes accounted for most of the L^{OH}, OFP, and SOAP, thus, these 2 kinds of VOCs
should get more priority in emission reduction policies and strategies. During all the seasons, the study
435 area was in the VOC-sensitive regime for O₃ formation. Therefore, VOCs especially aromatics and
alkenes emission reduction is the most effective way to decrease the local O₃ formation.

Data availability

All the data presented in this article can be accessed through <https://osf.io/bm6cs/>.

440

Author contribution

YLZ designed and supervised the project; MYF, FX, YCL, FC, and AM conducted the measurements;
AM analysed the data and prepared the manuscript. All authors contributed in discussion to improve the
article.

445

Competing interests

The authors declare that they have no conflict of interest.

Acknowledgements

450 The authors thank funding support from the National Nature Science Foundation of China (No.
41977305 and 41761144056), the Provincial Natural Science Foundation of Jiangsu (No.
BK20180040), and the Jiangsu Innovation & Entrepreneurship Team. We are also grateful to Zijin
Zhang and Meng-Yao Cao for their help on sampling.

References

455 Akagi, S. K., Yokelson, R. J., Wiedinmyer, C., Alvarado, M. J., Reid, J. S., Karl, T., ... Wennberg, P.



- O. (2011). Emission factors for open and domestic biomass burning for use in atmospheric models. *Atmospheric Chemistry and Physics*, 11(9), 4039–4072. <https://doi.org/10.5194/acp-11-4039-2011>
- An, J., Wang, J., Zhang, Y., & Zhu, B. (2017). Source Apportionment of Volatile Organic Compounds in an Urban Environment at the Yangtze River Delta, China. *Archives of Environmental Contamination and Toxicology*, 72(3), 335–348. <https://doi.org/10.1007/s00244-017-0371-3>
- 460 An, J., Zhu, B., Wang, H., Li, Y., Lin, X., & Yang, H. (2014a). Characteristics and source apportionment of VOCs measured in an industrial area of Nanjing, Yangtze River Delta, China. *Atmospheric Environment*, 97, 206–214. <https://doi.org/10.1016/j.atmosenv.2014.08.021>
- An, J., Zhu, B., Wang, H., Li, Y., Lin, X., & Yang, H. (2014b). Characteristics and source
465 apportionment of VOCs measured in an industrial area of Nanjing, Yangtze River Delta, China. *Atmospheric Environment*, 97, 206–214. <https://doi.org/10.1016/j.atmosenv.2014.08.021>
- An, J., Zou, J., Wang, J., Lin, X., & Zhu, B. (2015). Differences in ozone photochemical characteristics between the megacity Nanjing and its suburban surroundings, Yangtze River Delta, China.
470 *Environmental Science and Pollution Research*, 22(24), 19607–19617. <https://doi.org/10.1007/s11356-015-5177-0>
- Cardelino, C. A., & Chameides, W. L. (1995). An observation-based model for analyzing ozone precursor relationships in the urban atmosphere. *Journal of the Air and Waste Management Association*, 45(3), 161–180. <https://doi.org/10.1080/10473289.1995.10467356>
- 475 Carter, W. P. L. (2010). Development of the SAPRC-07 chemical mechanism. *Atmospheric Environment*, 44(40), 5324–5335. <https://doi.org/10.1016/j.atmosenv.2010.01.026>
- Chen, Y., Ge, X., Chen, H., Xie, X., Chen, Y., Wang, J., ... Chen, M. (2018). Seasonal light absorption properties of water-soluble brown carbon in atmospheric fine particles in Nanjing, China. *Atmospheric Environment*, 187(June), 230–240. <https://doi.org/10.1016/j.atmosenv.2018.06.002>
- 480 Deng, Y., Li, J., Li, Y., Wu, R., & Xie, S. (2019). Characteristics of volatile organic compounds, NO₂, and effects on ozone formation at a site with high ozone level in Chengdu. *Journal of Environmental Sciences (China)*, 75(2), 334–345. <https://doi.org/10.1016/j.jes.2018.05.004>
- Derwent, R. G., Jenkin, M. E., Utembe, S. R., Shallcross, D. E., Murrells, T. P., & Passant, N. R.



- (2010). Secondary organic aerosol formation from a large number of reactive man-made organic
485 compounds. *Science of the Total Environment*, 408(16), 3374–3381.
<https://doi.org/10.1016/j.scitotenv.2010.04.013>
- Feng, R., Wang, Q., Huang, C. chen, Liang, J., Luo, K., Fan, J. ren, & Zheng, H. jun. (2019). Ethylene,
xylene, toluene and hexane are major contributors of atmospheric ozone in Hangzhou, China, prior
to the 2022 Asian Games. *Environmental Chemistry Letters*, 17(2), 1151–1160.
490 <https://doi.org/10.1007/s10311-018-00846-w>
- Feng, T., Bei, N., Huang, R. J., Cao, J., Zhang, Q., Zhou, W., ... Li, G. (2016). Summertime ozone
formation in Xi'an and surrounding areas, China. *Atmospheric Chemistry and Physics*, 16(7),
4323–4342. <https://doi.org/10.5194/acp-16-4323-2016>
- He, Z., Wang, X., Ling, Z., Zhao, J., Guo, H., Shao, M., & Wang, Z. (2019). Contributions of different
495 anthropogenic volatile organic compound sources to ozone formation at a receptor site in the Pearl
River Delta region and its policy implications. *Atmospheric Chemistry and Physics*, 19(13), 8801–
8816. <https://doi.org/10.5194/acp-19-8801-2019>
- Hoshi, J., Amano, S., Sasaki, Y., & Korenaga, T. (2008). Investigation and estimation of emission
sources of 54 volatile organic compounds in ambient air in Tokyo. *Atmospheric Environment*,
500 42(10), 2383–2393. <https://doi.org/https://doi.org/10.1016/j.atmosenv.2007.12.024>
- Huang, X., Wang, C., Zhu, B., Lin, L., & He, L. (2019). Exploration of sources of OVOCs in various
atmospheres in southern. *Environmental Pollution*, 249, 831–842.
<https://doi.org/10.1016/j.envpol.2019.03.106>
- Hui, L., Liu, X., Tan, Q., Feng, M., An, J., Qu, Y., ... Cheng, N. (2019). VOC characteristics, sources
505 and contributions to SOA formation during haze events in Wuhan, Central China. *Science of the
Total Environment*, 650, 2624–2639. <https://doi.org/10.1016/j.scitotenv.2018.10.029>
- Hui, L., Liu, X., Tan, Q., Feng, M., An, J., Qu, Y., ... Jiang, M. (2018a). Characteristics, source
apportionment and contribution of VOCs to ozone formation in Wuhan, Central China.
Atmospheric Environment, 192(August), 55–71. <https://doi.org/10.1016/j.atmosenv.2018.08.042>
- 510 Hui, L., Liu, X., Tan, Q., Feng, M., An, J., Qu, Y., ... Jiang, M. (2018b). Characteristics, source
apportionment and contribution of VOCs to ozone formation in Wuhan, Central China.



- Atmospheric Environment*, 192(2), 55–71. <https://doi.org/10.1016/j.atmosenv.2018.08.042>
- Hung-Lung, C., Jiun-Horng, T., Shih-Yu, C., Kuo-Hsiung, L., & Sen-Yi, M. (2007). VOC concentration profiles in an ozone non-attainment area: A case study in an urban and industrial complex metroplex in southern Taiwan. *Atmospheric Environment*, 41(9), 1848–1860. <https://doi.org/10.1016/j.atmosenv.2006.10.055>
- Jenkin, M. E., Young, J. C., & Rickard, A. R. (2015). The MCM v3.3.1 degradation scheme for isoprene. *Atmospheric Chemistry and Physics*, 15(20), 11433–11459. <https://doi.org/10.5194/acp-15-11433-2015>
- Jenkin, Michael E., Saunders, S. M., & Pilling, M. J. (1997). The tropospheric degradation of volatile organic compounds: A protocol for mechanism development. *Atmospheric Environment*, 31(1), 81–104. [https://doi.org/10.1016/S1352-2310\(96\)00105-7](https://doi.org/10.1016/S1352-2310(96)00105-7)
- Jia, C., Mao, X., Huang, T., Liang, X., Wang, Y., Shen, Y., ... Gao, H. (2016). Non-methane hydrocarbons (NMHCs) and their contribution to ozone formation potential in a petrochemical industrialized city, Northwest China. *Atmospheric Research*, 169, 225–236. <https://doi.org/10.1016/j.atmosres.2015.10.006>
- Kumar, A., Singh, D., Kumar, K., Singh, B. B., & Jain, V. K. (2018). Distribution of VOCs in urban and rural atmospheres of subtropical India: Temporal variation, source attribution, ratios, OFP and risk assessment. *Science of the Total Environment*, 613–614, 492–501. <https://doi.org/10.1016/j.scitotenv.2017.09.096>
- Li, B., Sai, S., Ho, H., Gong, S., Ni, J., Li, H., ... Qi, Y. (2019). Characterization of VOCs and their related atmospheric processes in a central Chinese city during severe ozone pollution periods, 617–638.
- Li, C., Li, Q., Tong, D., Wang, Q., Wu, M., Sun, B., ... Tan, L. (2020). Environmental impact and health risk assessment of volatile organic compound emissions during different seasons in Beijing. *Journal of Environmental Sciences (China)*, 93, 1–12. <https://doi.org/10.1016/j.jes.2019.11.006>
- Li, J., Xie, S. D., Zeng, L. M., Li, L. Y., Li, Y. Q., & Wu, R. R. (2015). Characterization of ambient volatile organic compounds and their sources in Beijing, before, during, and after Asia-Pacific Economic Cooperation China 2014. *Atmospheric Chemistry and Physics*, 15(14), 7945–7959.



- 540 <https://doi.org/10.5194/acp-15-7945-2015>
- Li, Jing, Zhai, C., Yu, J., Liu, R., Li, Y., Zeng, L., & Xie, S. (2018). Spatiotemporal variations of ambient volatile organic compounds and their sources in Chongqing, a mountainous megacity in China. *Science of the Total Environment*, 627, 1442–1452. <https://doi.org/10.1016/j.scitotenv.2018.02.010>
- 545 Li, L., Xie, S., Zeng, L., Wu, R., & Li, J. (2015). Characteristics of volatile organic compounds and their role in ground-level ozone formation in the Beijing-Tianjin-Hebei region, China. *Atmospheric Environment*, 113, 247–254. <https://doi.org/10.1016/j.atmosenv.2015.05.021>
- Liu, B., Liang, D., Yang, J., Dai, Q., Bi, X., Feng, Y., ... Xu, H. (2016). Characterization and source apportionment of volatile organic compounds based on 1-year of observational data in Tianjin, China. *Environmental Pollution*, 218, 757–769. <https://doi.org/10.1016/j.envpol.2016.07.072>
- 550 Liu, Y., Wang, H., Jing, S., Gao, Y., Peng, Y., Lou, S., ... An, J. (2019). Characteristics and sources of volatile organic compounds (VOCs) in Shanghai during summer: Implications of regional transport. *Atmospheric Environment*, 215, 116902. <https://doi.org/10.1016/j.atmosenv.2019.116902>
- 555 Ma, Z., Liu, C., Zhang, C., Liu, P., Ye, C., Xue, C., ... Mu, Y. (2019). The levels, sources and reactivity of volatile organic compounds in a typical urban area of Northeast China. *Journal of Environmental Sciences*, 79, 121–134. <https://doi.org/10.1016/j.jes.2018.11.015>
- Meng, H. A. N., Xueqiang, L. U., Chunsheng, Z., Liang, R. A. N., & Suqin, H. A. N. (2015). Characterization and Source Apportionment of Volatile Organic Compounds in Urban and Suburban Tianjin, China. *Advances in Atmospheric Sciences*, 32(3), 439–444. <https://doi.org/10.1007/s00376-014-4077-4.1>
- 560 Mo, Z., Shao, M., Lu, S., Niu, H., Zhou, M., & Sun, J. (2017). Characterization of non-methane hydrocarbons and their sources in an industrialized coastal city, Yangtze River Delta, China. *Science of the Total Environment*, 593–594, 641–653. <https://doi.org/10.1016/j.scitotenv.2017.03.123>
- 565 Mozaffar, A., & Zhang, Y. L. (2020). Atmospheric Volatile Organic Compounds (VOCs) in China: a Review. *Current Pollution Reports*, 6(3), 250–263. <https://doi.org/10.1007/s40726-020-00149-1>



- Mozaffar, A., Zhang, Y. L., Fan, M., Cao, F., & Lin, Y. C. (2020). Characteristics of summertime ambient VOCs and their contributions to O₃ and SOA formation in a suburban area of Nanjing, China. *Atmospheric Research*, 240(February). <https://doi.org/10.1016/j.atmosres.2020.104923>
- Na, K., Kim, Y. P., Moon, K.-C., Moon, I., & Fung, K. (2001). Concentrations of volatile organic compounds in an industrial area of Korea. *Atmospheric Environment*, 35(15), 2747–2756. [https://doi.org/10.1016/S1352-2310\(00\)00313-7](https://doi.org/10.1016/S1352-2310(00)00313-7)
- Niu, Z., Zhang, H., Xu, Y., Liao, X., Xu, L., & Chen, J. (2012). Pollution characteristics of volatile organic compounds in the atmosphere of Haicang District in Xiamen City, Southeast China. *Journal of Environmental Monitoring*, 14(4), 1144–1151. <https://doi.org/10.1039/C2EM10884D>
- Petit, J. E., Favez, O., Albinet, A., & Canonaco, F. (2017). A user-friendly tool for comprehensive evaluation of the geographical origins of atmospheric pollution: Wind and trajectory analyses. *Environmental Modelling and Software*, 88, 183–187. <https://doi.org/10.1016/j.envsoft.2016.11.022>
- Saunders, S. M., Jenkin, M. E., Derwent, R. G., & Pilling, M. J. (2003). Protocol for the development of the Master Chemical Mechanism, MCM v3 (Part A): Tropospheric degradation of non-aromatic volatile organic compounds. *Atmospheric Chemistry and Physics*, 3(1), 161–180. <https://doi.org/10.5194/acp-3-161-2003>
- Shao, P., An, J., Xin, J., Wu, F., Wang, J., Ji, D., & Wang, Y. (2016). Source apportionment of VOCs and the contribution to photochemical ozone formation during summer in the typical industrial area in the Yangtze River Delta, China. *Atmospheric Research*, 176–177, 64–74. <https://doi.org/10.1016/j.atmosres.2016.02.015>
- Shi, J., Deng, H., Bai, Z., Kong, S., Wang, X., Hao, J., ... Ning, P. (2015). Emission and profile characteristic of volatile organic compounds emitted from coke production, iron smelt, heating station and power plant in Liaoning Province, China. *Science of the Total Environment*, 515–516(x), 101–108. <https://doi.org/10.1016/j.scitotenv.2015.02.034>
- Song, M., Li, X., Yang, S., Yu, X., Zhou, S., Yang, Y., ... Zhang, Y. (2020). Spatiotemporal Variation, Sources, and Secondary Transformation Potential of VOCs in Xi'an, China, 30(August). Retrieved from <https://doi.org/10.5194/acp-2020-704>



- Song, M., Tan, Q., Feng, M., Qu, Y., & Liu, X. (2018). Source Apportionment and Secondary Transformation of Atmospheric Nonmethane Hydrocarbons in Chengdu , Southwest China. *Journal of Geophysical Research Atmospheres*, 123(2), 9741–9763. <https://doi.org/10.1029/2018JD028479>
- 600 Song, M., Tan, Q., Feng, M., Qu, Y., Liu, X., An, J., & Zhang, Y. (2018). Source Apportionment and Secondary Transformation of Atmospheric Nonmethane Hydrocarbons in Chengdu, Southwest China. *Journal of Geophysical Research: Atmospheres*, 123(17), 9741–9763. <https://doi.org/10.1029/2018JD028479>
- Sun, J., Shen, Z., Zhang, Y., Zhang, Z., Zhang, Q., Zhang, T., ... Li, X. (2019). Urban VOC profiles, possible sources, and its role in ozone formation for a summer campaign over Xi'an, China. *Environmental Science and Pollution Research*, 26(27), 27769–27782. <https://doi.org/10.1007/s11356-019-05950-0>
- 605
- Tan, Z., Lu, K., Dong, H., Hu, M., Li, X., Liu, Y., ... Zhang, Y. (2018). Explicit diagnosis of the local ozone production rate and the ozone-NO_x-VOC sensitivities. *Science Bulletin*, 63(16), 1067–1076. <https://doi.org/10.1016/j.scib.2018.07.001>
- 610
- Tan, Z., Lu, K., Jiang, M., Su, R., Dong, H., Zeng, L., ... Zhang, Y. (2018a). Exploring ozone pollution in Chengdu, southwestern China: A case study from radical chemistry to O₃-VOC-NO_x sensitivity. *Science of The Total Environment*, 636, 775–786. <https://doi.org/10.1016/J.SCITOTENV.2018.04.286>
- 615
- Tan, Z., Lu, K., Jiang, M., Su, R., Dong, H., Zeng, L., ... Zhang, Y. (2018b). Exploring ozone pollution in Chengdu , southwestern China: A case study from radical chemistry to O₃-VOC-NO_x sensitivity. *Science of the Total Environment*, 636, 775–786. <https://doi.org/10.1016/j.scitotenv.2018.04.286>
- Tan, Z., Lu, K., Jiang, M., Su, R., Wang, H., Lou, S., ... Zhang, Y. (2019). Daytime atmospheric oxidation capacity in four Chinese megacities during the photochemically polluted season: A case study based on box model simulation. *Atmospheric Chemistry and Physics*, 19(6), 3493–3513. <https://doi.org/10.5194/acp-19-3493-2019>
- 620
- Tang, J. H., Chan, L. Y., Chan, C. Y., Li, Y. S., Chang, C. C., Liu, S. C., ... Li, Y. D. (2007).



- 625 Characteristics and diurnal variations of NMHCs at urban, suburban, and rural sites in the Pearl
River Delta and a remote site in South China. *Atmospheric Environment*, 41(38), 8620–8632.
<https://doi.org/https://doi.org/10.1016/j.atmosenv.2007.07.029>
- Tiwari, V., Hanai, Y., & Masunaga, S. (2010). Ambient levels of volatile organic compounds in the
vicinity of petrochemical industrial area of Yokohama, Japan. *Air Quality, Atmosphere and Health*,
3(2), 65–75. <https://doi.org/10.1007/s11869-009-0052-0>
- 630 Vermeuel, M. P., Novak, G. A., Alwe, H. D., Hughes, D. D., Kaleel, R., Dickens, A. F., ... Bertram, T.
H. (2019). Sensitivity of Ozone Production to NO_x and VOC Along the Lake Michigan Coastline.
Journal of Geophysical Research: Atmospheres, 124(20), 10989–11006.
<https://doi.org/10.1029/2019JD030842>
- von Schneidemesser, E., Monks, P. S., & Plass-Duelmer, C. (2010). Global comparison of VOC and
635 CO observations in urban areas. *Atmospheric Environment*, 44(39), 5053–5064.
<https://doi.org/10.1016/j.atmosenv.2010.09.010>
- Wang, S., Wei, W., Du, L., Li, G., & Hao, J. (2009). Characteristics of gaseous pollutants from biofuel-
stoves in rural China. *Atmospheric Environment*, 43(27), 4148–4154.
<https://doi.org/10.1016/j.atmosenv.2009.05.040>
- 640 Warneke, C., De Gouw, J. A., Holloway, J. S., Peischl, J., Ryerson, T. B., Atlas, E., ... Parrish, D. D.
(2012). Multiyear trends in volatile organic compounds in Los Angeles, California: Five decades
of decreasing emissions. *Journal of Geophysical Research Atmospheres*, 117(17), 1–10.
<https://doi.org/10.1029/2012JD017899>
- Wolfe, G. M., Marvin, M. R., Roberts, S. J., Travis, K. R., & Liao, J. (2016). The framework for 0-D
645 atmospheric modeling (F0AM) v3.1. *Geoscientific Model Development*, 9(9), 3309–3319.
<https://doi.org/10.5194/gmd-9-3309-2016>
- Wu, R., Zhao, Y., Zhang, J., & Zhang, L. (2020). Variability and sources of ambient volatile organic
compounds based on online measurements in a suburban region of nanjing, eastern China. *Aerosol
and Air Quality Research*, 20(3), 606–619. <https://doi.org/10.4209/aaqr.2019.10.0517>
- 650 Xu, Z., Huang, X., Nie, W., Chi, X., & Xu, Z. (2017). Influence of synoptic condition and holiday
effects on VOCs and ozone production in the Yangtze River Delta region , China. *Atmospheric*



- Environment*, 168, 112–124. <https://doi.org/10.1016/j.atmosenv.2017.08.035>
- 655 Yan, Y., Yang, C., Peng, L., Li, R., & Bai, H. (2016). Emission characteristics of volatile organic compounds from coal-, coal gangue-, and biomass-fired power plants in China. *Atmospheric Environment*, 143, 261–269. <https://doi.org/10.1016/j.atmosenv.2016.08.052>
- Yoshino, A., Nakashima, Y., Miyazaki, K., Kato, S., Suthawaree, J., Shimo, N., ... Kajii, Y. (2012). Air quality diagnosis from comprehensive observations of total OH reactivity and reactive trace species in urban central Tokyo. *Atmospheric Environment*, 49, 51–59. <https://doi.org/10.1016/j.atmosenv.2011.12.029>
- 660 Zeng, P., Lyu, X. P., Guo, H., Cheng, H. R., Jiang, F., Pan, W. Z., ... Hu, Y. Q. (2018). Causes of ozone pollution in summer in Wuhan, Central China. *Environmental Pollution*, 241(x), 852–861. <https://doi.org/10.1016/j.envpol.2018.05.042>
- Zhang, F., Shang, X., Chen, H., Xie, G., Fu, Y., Wu, D., ... Chen, J. (2020). Significant impact of coal combustion on VOCs emissions in winter in a North China rural site. *Science of the Total Environment*, 720. <https://doi.org/10.1016/j.scitotenv.2020.137617>
- 665 Zhang, H., Li, H., Zhang, Q., Zhang, Y., Zhang, W., Wang, X., ... Xia, F. (2017). Atmospheric volatile organic compounds in a typical urban area of Beijing: Pollution characterization, health risk assessment and source apportionment. *Atmosphere*, 8(3). <https://doi.org/10.3390/atmos8030061>
- Zhang, Yanli, Wang, X., Zhang, Z., Lü, S., Shao, M., Lee, F. S. C., & Yu, J. (2013). Species profiles and normalized reactivity of volatile organic compounds from gasoline evaporation in China. *Atmospheric Environment*, 79, 110–118. <https://doi.org/10.1016/j.atmosenv.2013.06.029>
- 670 Zhang, Yunchen, Li, R., Fu, H., Zhou, D., & Chen, J. (2018). Observation and analysis of atmospheric volatile organic compounds in a typical petrochemical area in Yangtze River. *Journal of Environmental Sciences*, 71, 233–248. <https://doi.org/10.1016/j.jes.2018.05.027>
- Zhang, Z., Yan, X., Gao, F., Thai, P., Wang, H., Chen, D., ... Wang, B. (2018). Emission and health risk assessment of volatile organic compounds in various processes of a petroleum refinery in the Pearl River Delta. *Environmental Pollution*, 238, 452–461. <https://doi.org/10.1016/j.envpol.2018.03.054>



- 680 Zhao, R., Dou, X., Zhang, N., Zhao, X., Yang, W., Han, B., ... Bai, Z. (2020). The characteristics of inorganic gases and volatile organic compounds at a remote site in the Tibetan Plateau. *Atmospheric Research*, 234(October 2019), 104740. <https://doi.org/10.1016/j.atmosres.2019.104740>
- 685 Zhu, J., Wang, S., Wang, H., Jing, S., Lou, S., Saiz-Lopez, A., & Zhou, B. (2019). Observationally constrained modelling of atmospheric oxidation capacity and photochemical reactivity in Shanghai, China. *Atmospheric Chemistry and Physics Discussions*, 1–26. <https://doi.org/10.5194/acp-2019-711>
- Zou, Y., Deng, X. J., Zhu, D., Gong, D. C., Wang, H., Li, F., ... Wang, B. G. (2015). Characteristics of 1 year of observational data of VOCs, NO_x and O₃ at a suburban site in Guangzhou, China. *Atmospheric Chemistry and Physics*, 15(12), 6625–6636. <https://doi.org/10.5194/acp-15-6625-2015>
- 690

695

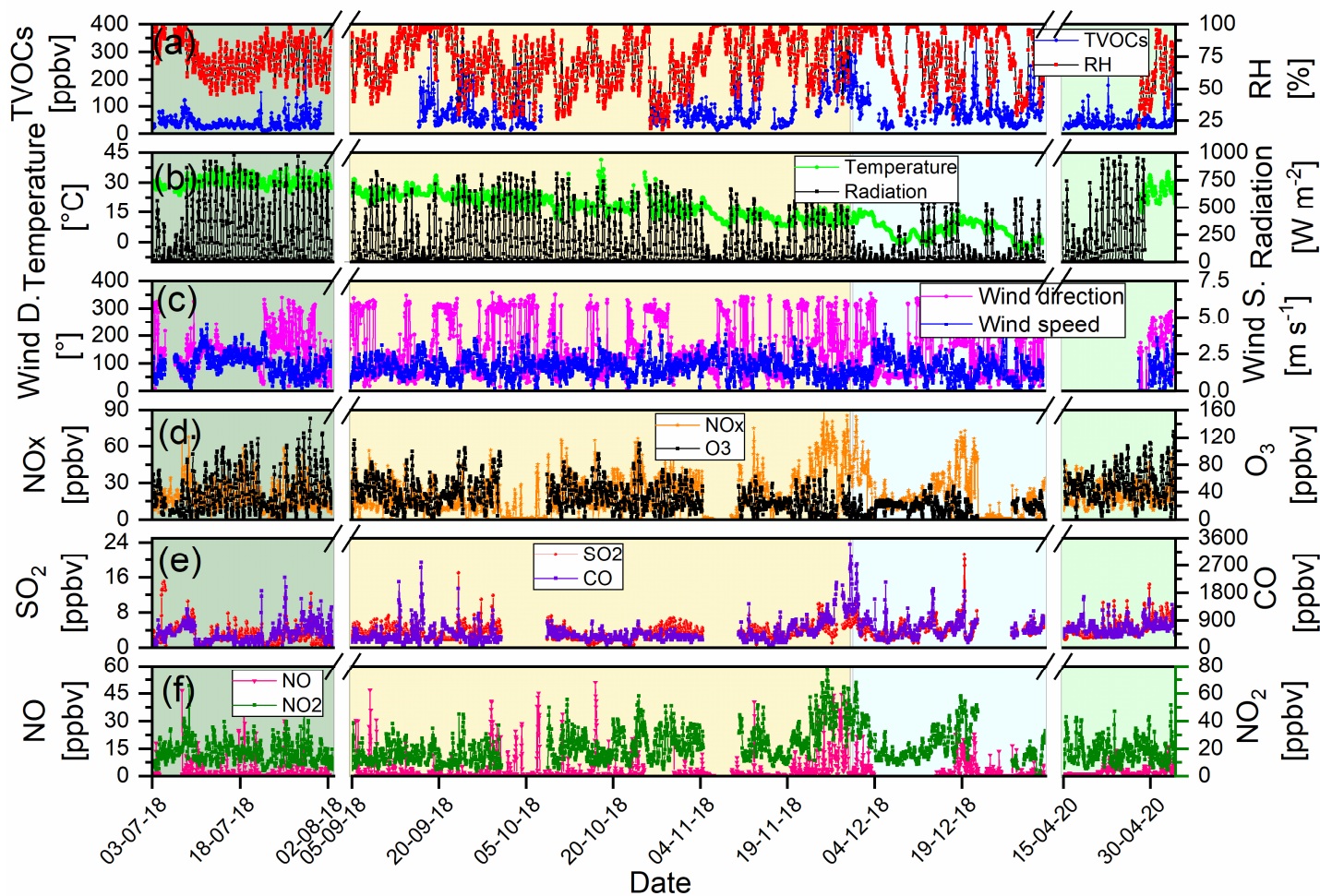


Figure 1: Time series of hourly meteorological parameters, inorganic air pollutants, and TVOCs concentrations during the observation period at Nanjing. The green, yellow, cyan, and light-green shaded areas indicate summer, autumn, winter, and spring seasons, respectively. The discontinuity of the measured data is due to the instruments failure.

700

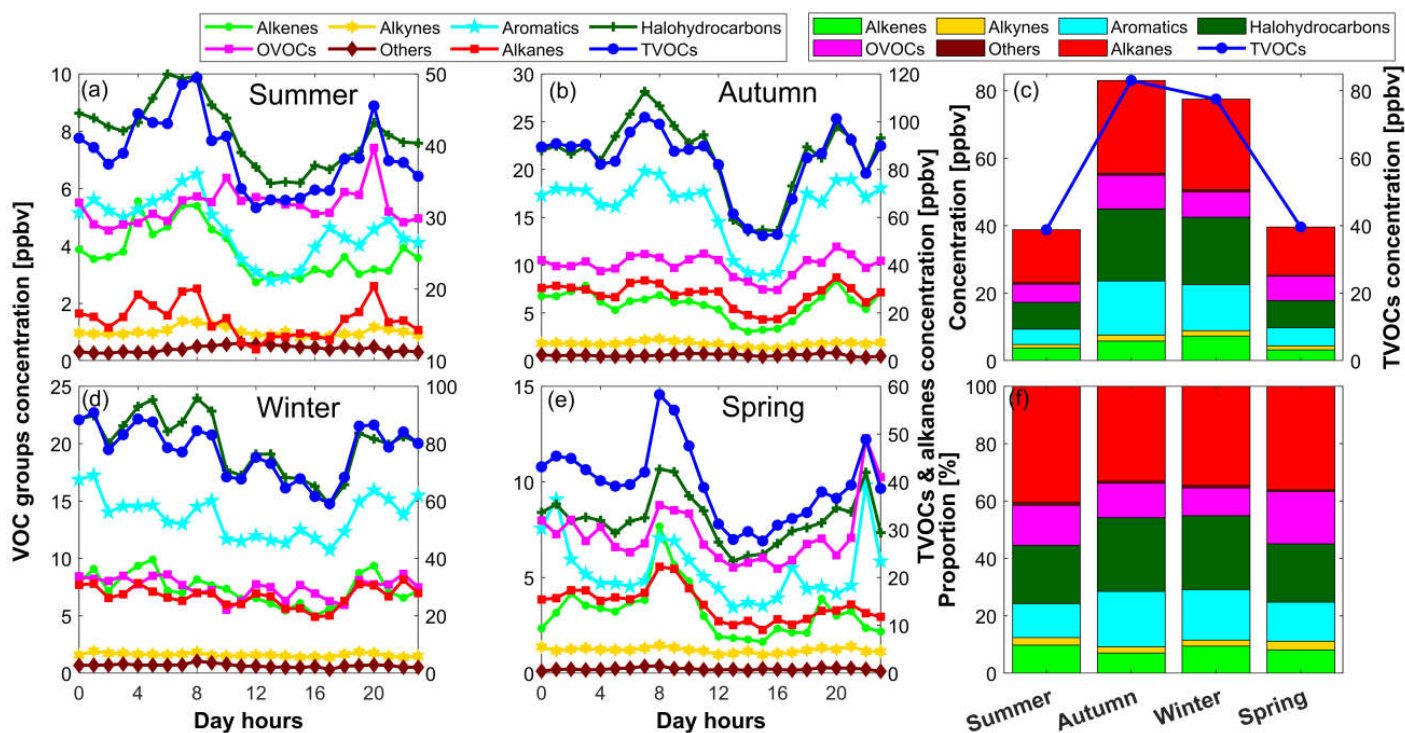


Figure 2: Diurnal variations in TVOCs and different VOC-groups concentrations in different seasons (a, b, d, & e) and seasonal variations in average concentrations and proportion of TVOCs and different VOC-groups (c & f).

705

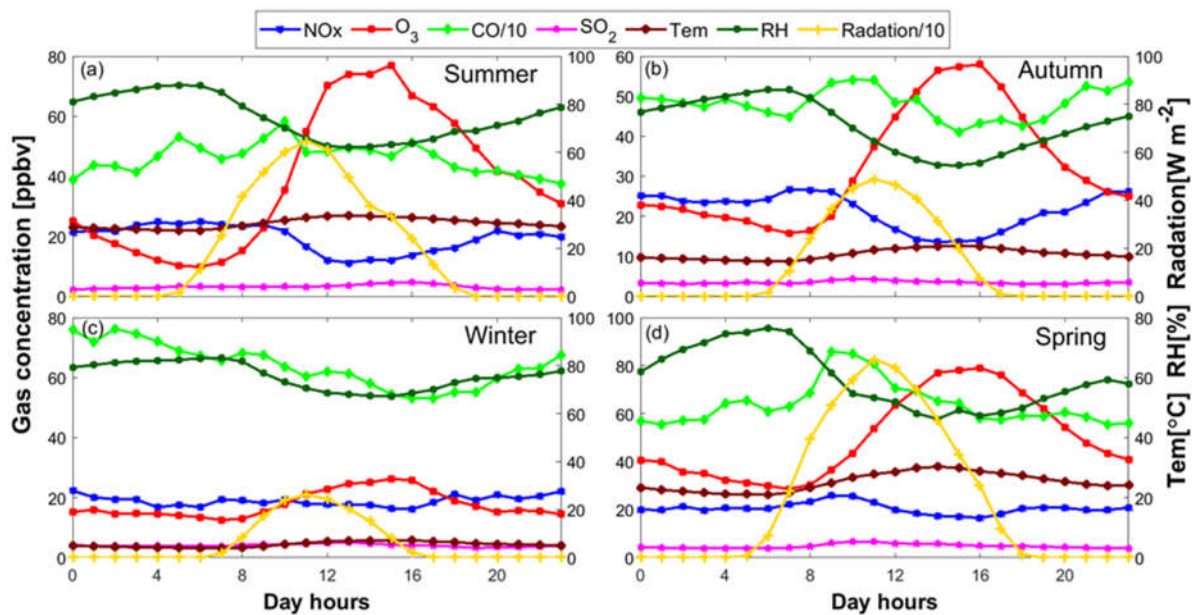


Figure 3: Diurnal variations in weather conditions and NO_x, O₃, CO, and SO₂ concentrations in different seasons. Note that the plotted CO concentrations and solar radiation values are reduced by 10-folds for a better visualization.

710

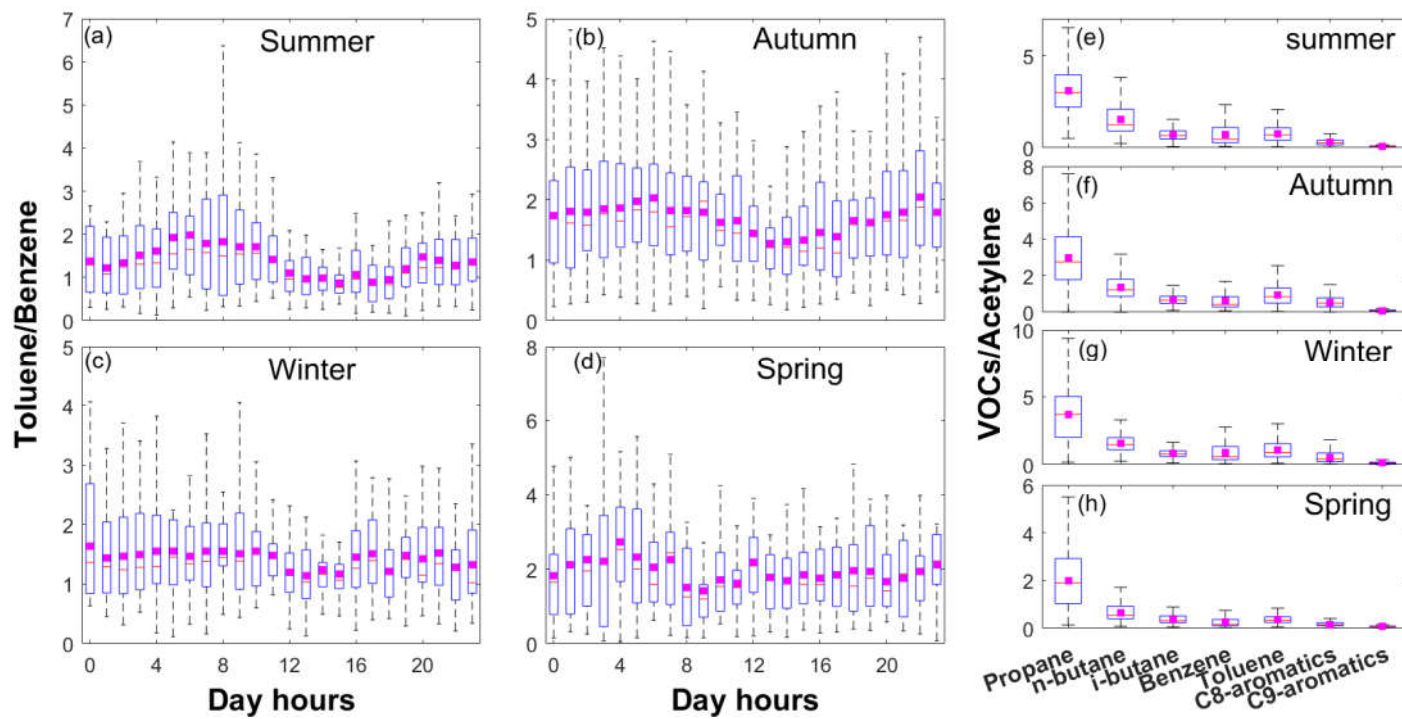


Figure 4: Diurnal variations in toluene/benzene ratios (a, b, c, & d) and in the ratios of different VOCs to acetylene in different seasons (e, f, g, & h). The pink-colored squares in the box-plots

715 represent the average values.

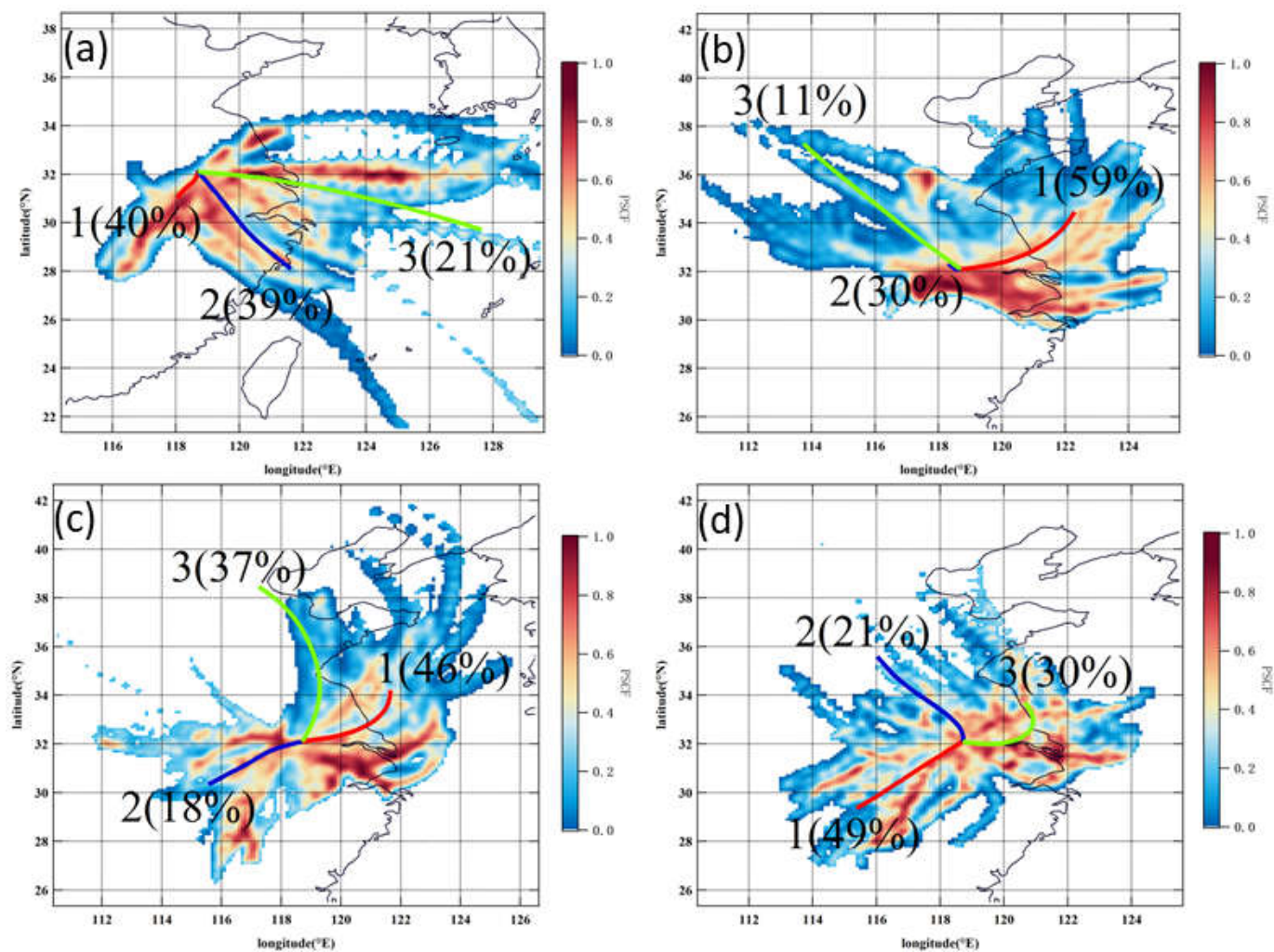
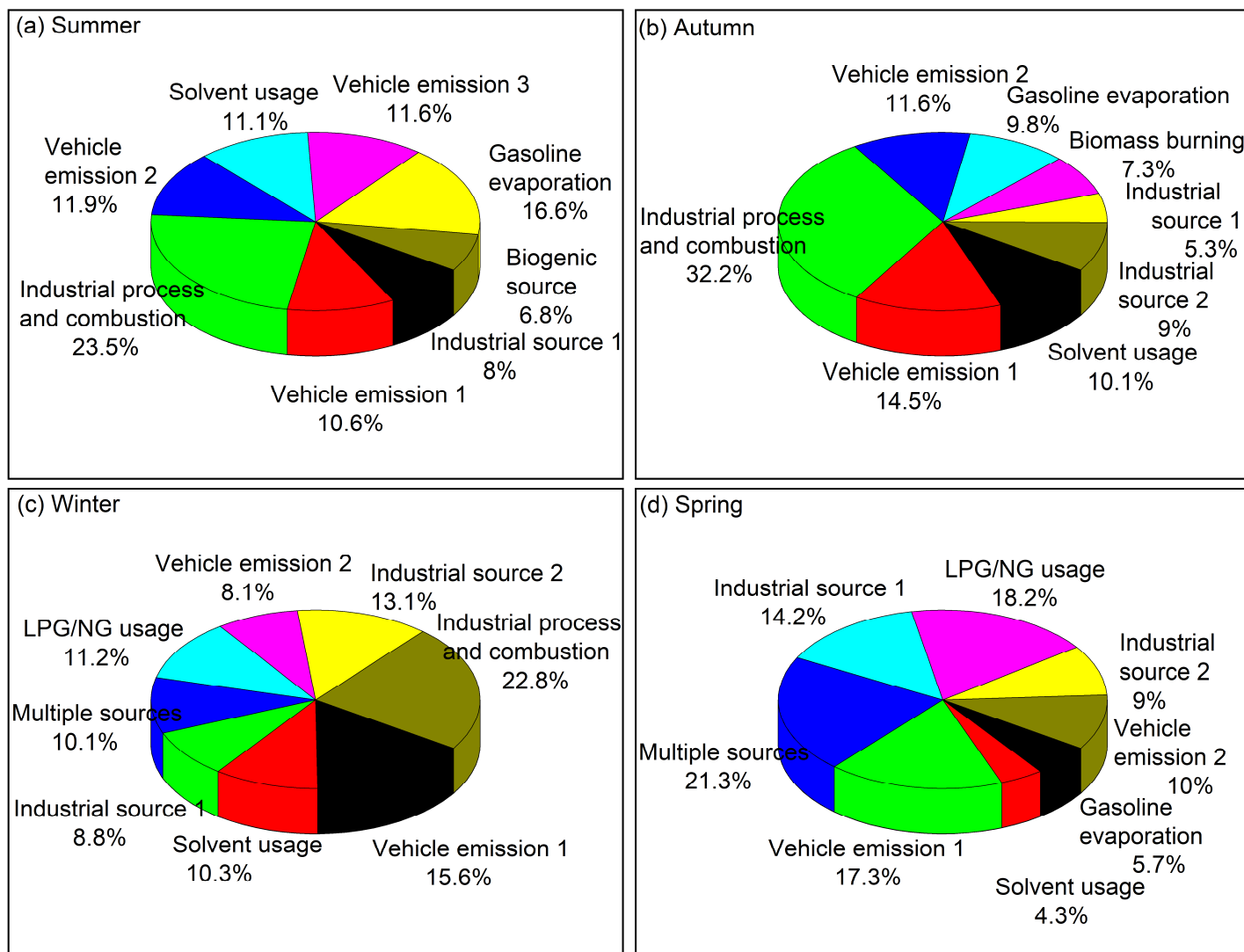


Figure 5: Wind cluster and PSCF analysis during (a) summer (b) autumn, (c) winter, and (d) spring based on the 24 hours backward air mass trajectories from the study area.



720 **Figure 6: relative contributions of different sources to ambient VOCs in Nanjing industrial area during different seasons**

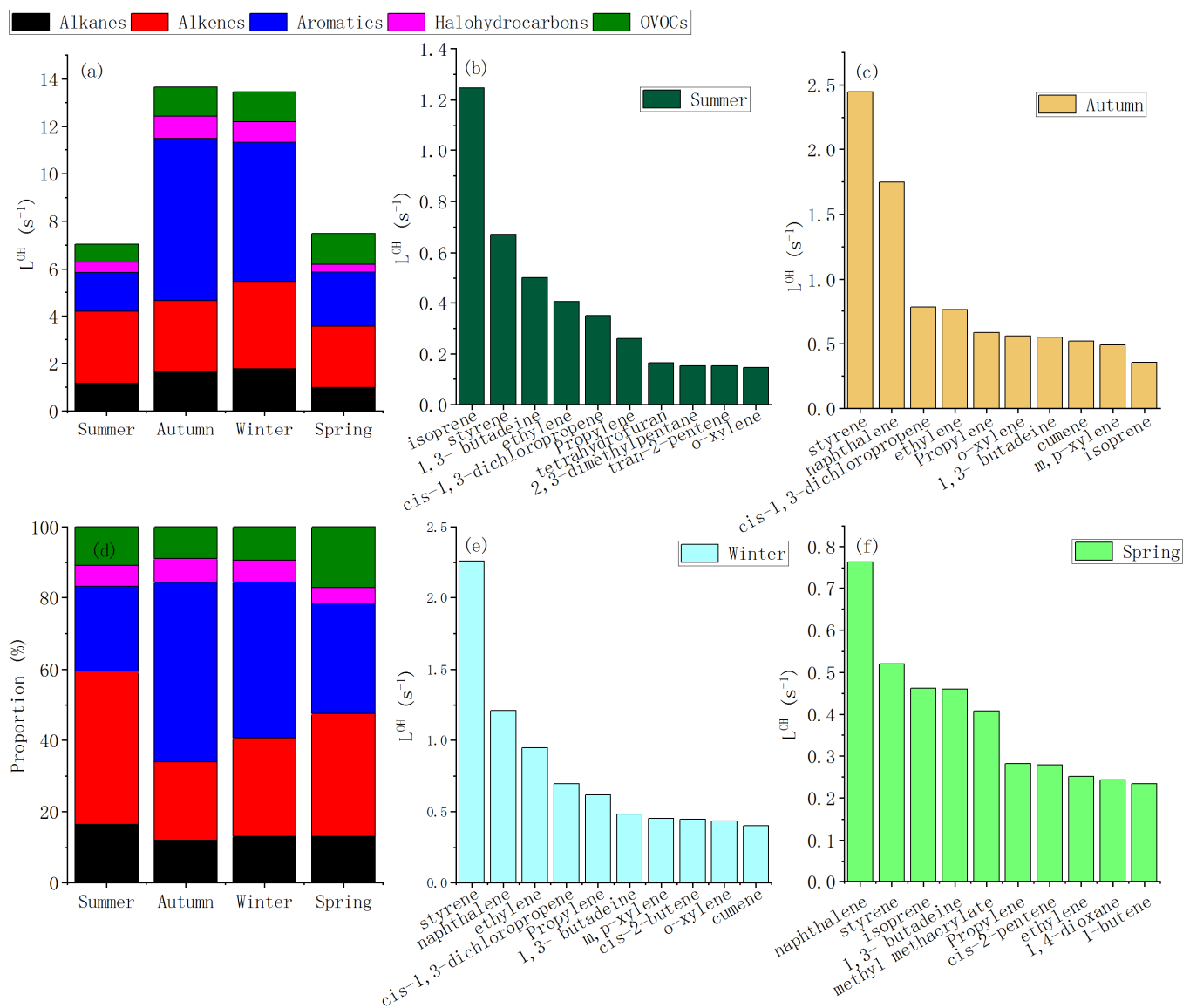


Figure 7: Contribution to OH loss rates of different VOC-groups and the top 10 VOC species in different seasons

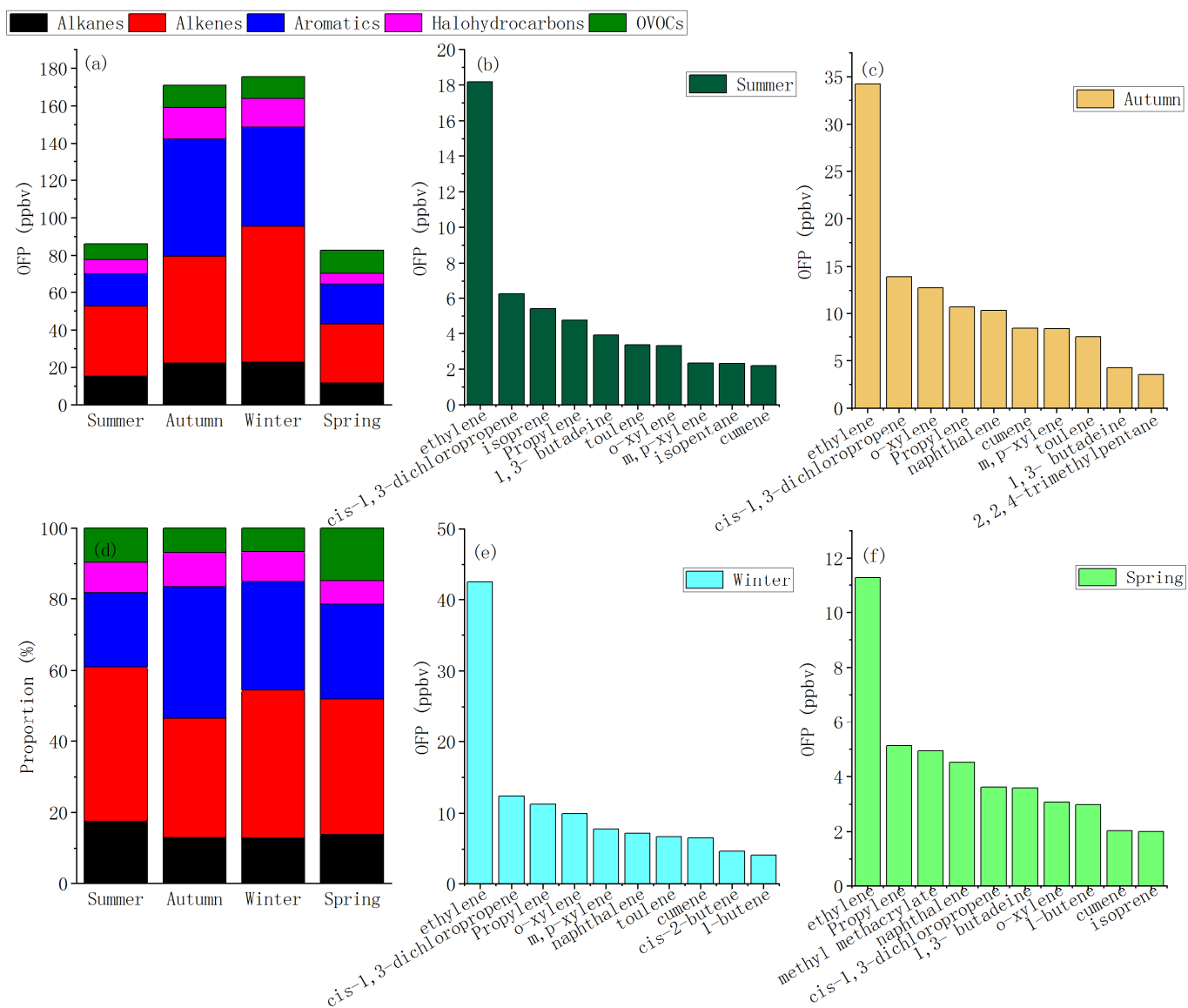


Figure 8: Contribution to ozone formation potential of different VOC-groups and the top 10 VOC species in different seasons

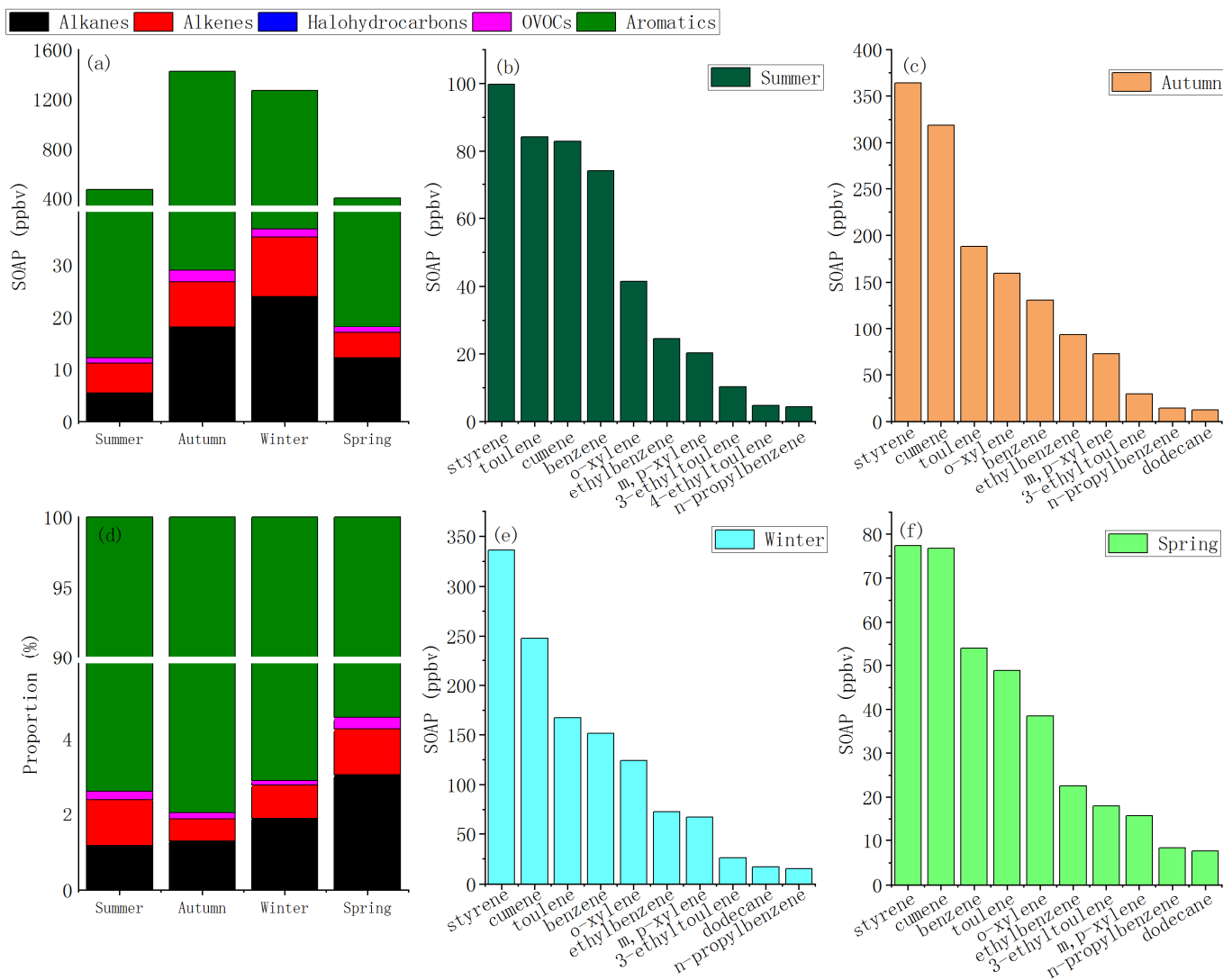
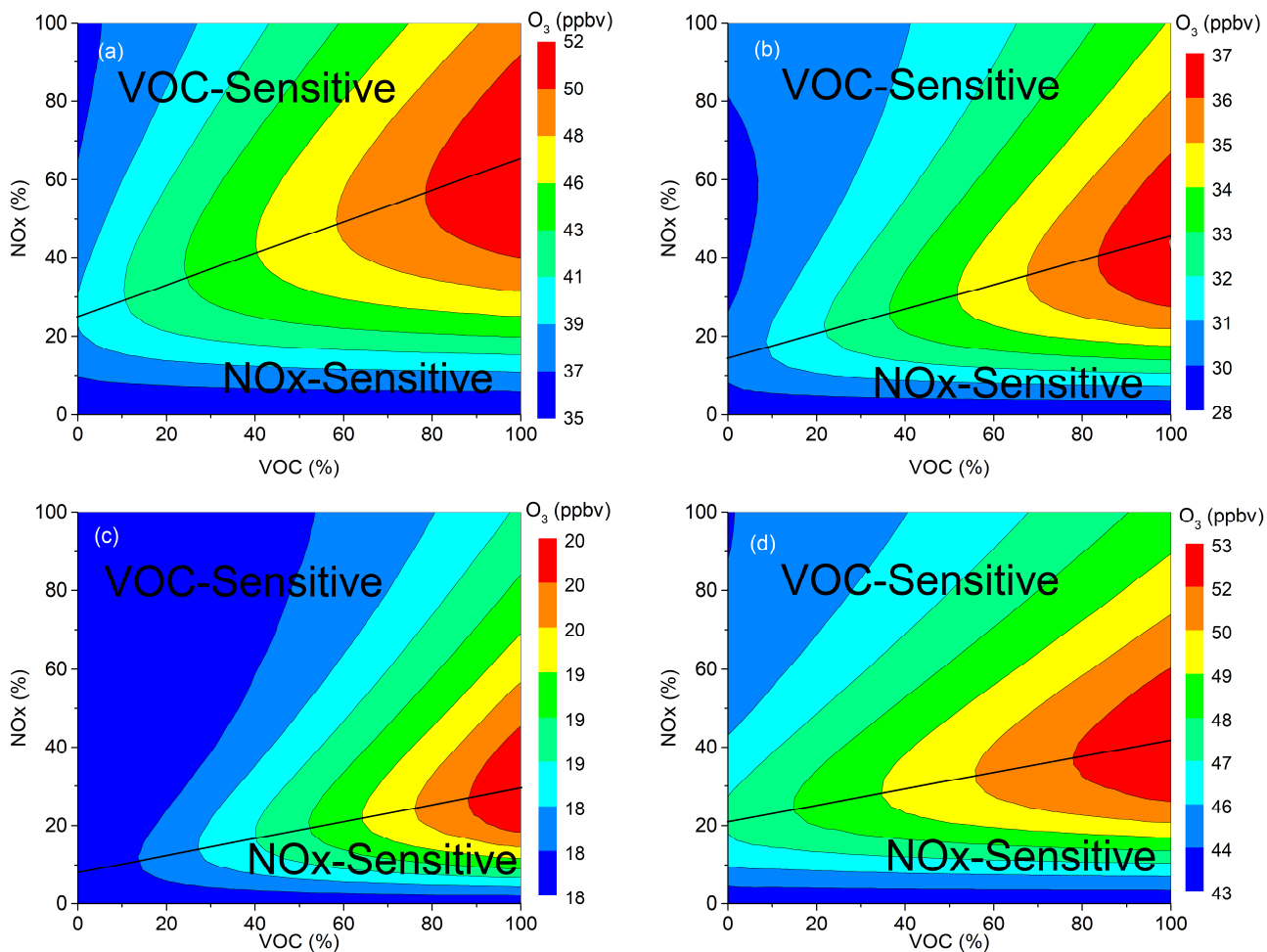
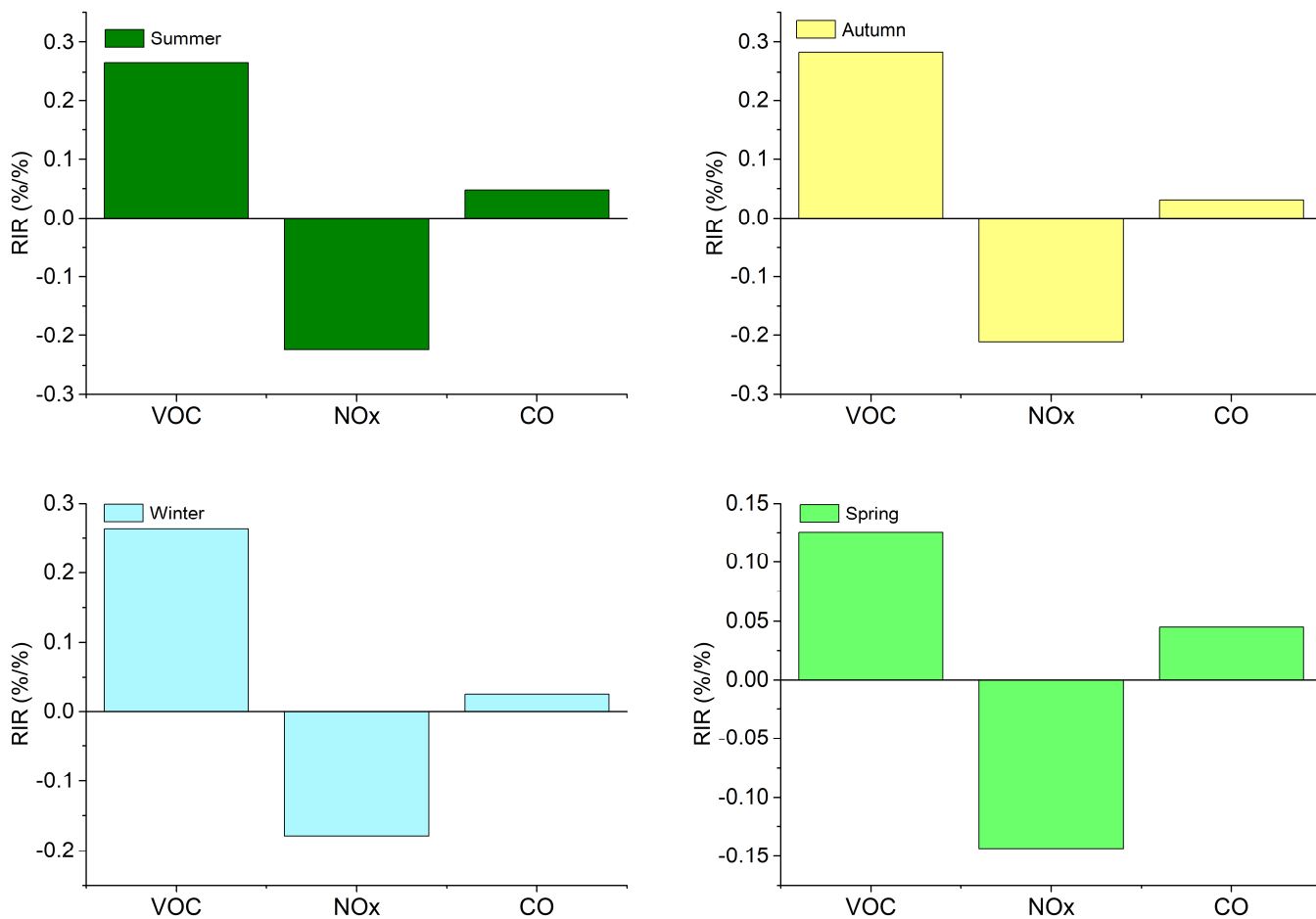


Figure 9: Contribution to secondary organic aerosol formation potential of different VOC-groups and the top 10 VOC species in different seasons



735

Figure 10: O₃ isopleth diagram for (a) summer (b) autumn, (c) winter, and (d) spring based on percentage changes in VOCs and NO_x concentrations in Nanjing and corresponding modelled O₃ production.



740

Figure 11: The RIR values of the VOC, NO_x, and CO for the different seasons in Nanjing